

GT2011-46) \$-

EFFECTS DUE TO THE TEMPERATURE MEASUREMENT SECTION ON THE PERFORMANCE ESTIMATION OF A CENTRIFUGAL COMPRESSOR STAGE

Alessandro Bianchini **Giovanni Ferrara** **Lorenzo Ferrari**
 "Sergio Stecco" Department of Energy Engineering, University of Florence, Florence, Italy
 Tel. +39 055 4796570 - Fax +39 055 4796342 - E-mail ferrari@vega.de.unifi.it

Valeria Ballarini **Lorenzo Bianchi** **Libero Tapinassi** **Lorenzo Toni**
 GE Oil & Gas, Florence, Italy
 Tel. +39 055 423 3151 - Fax +39 055 423 2800 - E-mail lorenzo.bianchi@ge.com

ABSTRACT

A wide-ranging analysis was performed by *GE Oil & Gas* and the University of Florence to investigate the effects on the estimation of centrifugal compressor performance induced by a different choice of the total temperature measurement section. With this goal in mind, the study focused on the analysis of a commonly found discrepancy between the measurements at the impeller outlet section and at the stage exit section.

Based on the experimental data collected on a centrifugal impeller, three main physical phenomena were analyzed and discussed in further detail. First the effect of the heat exchange was examined and its influence on the total temperature variation throughout the machine was extrapolated. Next, the influence of the heat-exchange phenomena affecting the temperature sensors was evaluated by means of numerical models and physical assumptions. Finally, the effects on the temperature measurement of the flow structure at the impeller outlet were investigated.

In particular, a corrective model to account for the thermal inertia of the thermocouples normally applied in this section was applied to the experimental data. The corrected temperatures at the investigated measurement sections were then compared and their influence on the correct stage performance estimation is discussed in this study.

NOMENCLATURE

A	Area	[m ²]
DC	Discharge Coeff.	
E	Energy	[J]
Ma	Mach Number	
Nu	Nusselt Number	
Pr	Prandtl Number	
R	Gas Constant	[J/(kg·K)]

Re	Reynolds Number	
T	Temperature	[K]
U	Tangential Velocity	[m/s]
V	Generic Velocity	[m/s]
W	Relative Velocity	[m/s]
X	Sensor Shape Coeff.	
c	Absolute velocity	[m/s]
c_p	Specific Heat Capacity	[J/(kg·K)]
d_w	Sensing Elem. Diameter	[m]
f	Friction factor	
h	Enthalpy	[J]
h_C	Convective Heat Coeff.	[W/(m ² ·K)]
k	Thermal Conductivity	[W/(m·K)]
l_w	Sensing Elem. Length	[m]
\dot{m}	Mass Flow Rate	[kg/s]
p	Pressure	[Pa]
r	Recovery Factor	
t	Time	[s]

Greek letters

β	Head Coefficient	
γ	Heat Capacities Ratio	
ε	Relative Wake Area	
η_P	Polytrophic Efficiency	
ξ	Rothalpy Loss Coefficient	
ρ	Density	[kg/m ³]
σ	Slip Factor	
τ	Work Coefficient	
φ	Flow Coefficient	

Subscripts

0	Total Quantity (Temperature or Pressure)
I	Generic Inlet Section

2	Generic Outlet Section
<i>cond</i>	Conductive
<i>DES</i>	Design
<i>gas</i>	Flowing gas
<i>i</i>	Generic element
<i>j</i>	Jet
<i>kin</i>	Kinetic
<i>MA</i>	Mass-averaged
<i>MAX</i>	Maximum
<i>MIN</i>	Minimum
<i>{R}</i>	Rack
<i>REF</i>	Reference value
<i>s</i>	Sensor
<i>stem</i>	Stem of the probe
<i>TA</i>	Time-averaged
<i>tot</i>	Total
<i>u</i>	Peripheral
<i>w</i>	Wake
<i>wire</i>	Wire (Thermocouple)
<i>ω</i>	Rotoric Reference System

Superscripts

* Dimensionless value

INTRODUCTION

The experimental analysis of the performance of centrifugal compressor stages is widely exploited by manufactures and designers both for the validation of numerical predictions and for the characterization of new aerodynamic solutions. In particular, an in depth study was undertaken to increase the accuracy in the measurement of thermodynamic parameters during the experimental testing of the products; in addition, in order to promote the standardization of the testing protocols, specific activities were directed to establishing a current state of the tests themselves.

Within this context, synergistic efforts were devoted to investigating a measurement problem that was generally found in the bench testing of centrifugal compressors concerning the effects of the total temperature measurement section on the estimation of the stage performance. In detail, a wide-ranging analysis was conceived to investigate a commonly found discrepancy between the total temperature measurements at the impeller outlet section and at the stage exit section (e.g. [1]). In the past, the company had adopted the latter positioning as the reference measurement section in order to prevent the measurement itself from being disturbed by the complex flow pattern at the impeller outlet. Some relevant advantages could be reached, however, by considering the measurement section at the impeller outlet, particularly concerning the reduced influence of the heat exchanges between the flow and the case.

From a theoretical point of view, there is no reason for the existence of the total temperature difference here investigated if one assumes an adiabatic behavior of the system and no work exchange in the statoric components (i.e. the total enthalpy of the system is preserved) [2]. It is worth noticing, however, that

the existence of this discrepancy can not be ignored in measuring the performance of a machine due to the fact that a different choice in the measurement section has a significant impact on the calculation of the overall performance indicators.

If one considers the classical Busemann's theory [3], the work coefficient of the compressor, defined by Eq. 1, is indeed assumed to collapse into the well-known Eq. 2 with any choice of the outlet section considered (i.e. either the impeller outlet or the stage outlet): no influence of the temperature variation between the sections is in fact hypothesized. Furthermore, the polytropic efficiency (Eq. 3) is also altered if differences in the outlet total temperature derive from a different choice of the measurement section.

$$\tau = \frac{\Delta h_0}{U^2} = \frac{c_p(T_{02} - T_{01})}{U^2} \quad (1)$$

$$\tau = \sigma - \varphi_2 \cot \beta_2 \quad (2)$$

$$\eta_p = \frac{\gamma - 1}{\gamma} \left[\frac{\ln\left(\frac{p_{02}}{p_{01}}\right)}{\ln\left(\frac{T_{02}}{T_{01}}\right)} \right] \quad (3)$$

For example, the variations induced by the choice of the impeller outlet section (Section 20 in this study) or the stage outlet section (Section 60) in evaluating the polytropic efficiency of the compressor here investigated are presented in Figure 1 as a function of the dimensionless flow coefficient $\varphi^* = \varphi / \varphi_{DES}$.

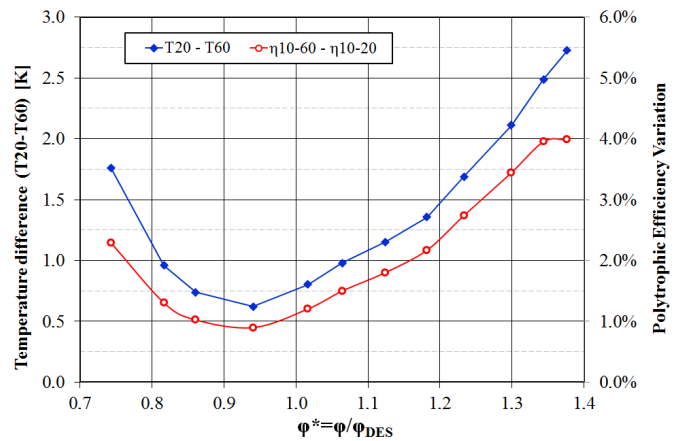


Figure 1 - Polypropy Efficiency Variations due to different choices in the evaluation of the outlet temperature.

METHODOLOGICAL APPROACH

In order to compare the results deriving from the two measurement sections, a combined theoretical and experimental approach was conceived. As a first step, a physical analysis of the problem was carried out; as a result, three main phenomena

were postulated as affecting the temperature measurement in the investigated sections:

- Heat exchange between the flow and the case along the flow path between the two sections (e.g. [4]);
- Kinetic and conductive measurement errors connected to the heat exchange between the sensing element and the stem (Manfrida et al. [1] and Bidini et al. [5]);
- Measurement error due to the thermal inertia of the thermocouple, whose frequency response is assumed to be inadequate for the investigation of an unstructured flow field such as that in the outlet of the impeller (i.e., with different flow velocities and total temperatures in the wake and jet zones) [6].

Each phenomenon was then theoretically analyzed using simplified models either extrapolated from the technical literature or suitably developed. The models were subsequently applied to the results of a series of experiments which were carried out in a test bench on a mixed-flow family impeller.

EXPERIMENTAL SETUP AND FACILITIES

The tests were performed in a specialized test rig at the *GE Oil & Gas Technology Laboratory (OGTL)* in Florence (Italy). The rig was operated in the closed-loop configuration with ambient pressure and temperature at the inlet of the stage; the gas utilized was air and the operating peripheral Mach number was equal to the design one ($Ma_u=0.85$). The inlet flow conditions in the stage are controlled with a heat exchanger; for more details on the rig facilities see Ferrara et al. [7].

The tested machine is an industrial “mixed flow” impeller for high-pressure applications with a very low axial component: the main features of the rotor are reported in Table 1. Figure 2 presents a schematic cross section of the stage, including the measurement sections, whose description and instrumentation setup are reported in Table 2, where the symbol {R} indicates a linear rack of 6 probes.

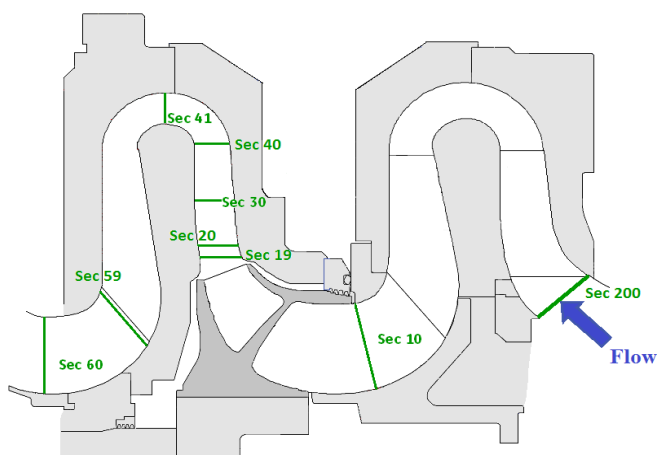


Figure 2 - Schematic cross section of the tested stage.

In particular, the experimental tests presented in our study were obtained with a pseudo-axial configuration.

All the probes and sensors used in the series of experiments were calibrated before each test in the metrological department of *GE Oil & Gas*, through a referenced process.

Focusing on the temperature measurements, the accuracy of the whole temperature measurement chain (i.e. the sensor, the reference junction and the digital multimeter), was measured in ± 0.2 K. As a result, in all the plots of this work, no error bands are added to the experimental points, as they are included in the data markers.

When multiple sensors are installed in each measurement section, the data are mass-averaged with respect to the entire flow field. In particular, the standard deviation among the thermocouple rakes, installed in the same section (but located in different tangential positions) was lower than 0.7 K.

Table 1 - Main features of the tested impeller.

MF 956 Centrifugal Impeller	
Impeller type	Mixed flow
Peripheral Mach Number (Ma_u)	0.85
Model scale	1:1

Table 2 - Definition of Measurement Sections.

Section	Total pressure	Static pressure	Total temperature	Flow direction
200	Kiel Probe	Wall tap	1x TC-J	-
10	1x {R} Kiel Probes	Wall tap	4x {R} TC-J	1x {R} Cobra Probes
19	-	Wall tap	-	-
20	FRAPP [8]	Wall tap	2x TC-J	1x 5-hole
30	-	-	2x TC-J	-
40	-	Wall tap	-	1x 3-hole
41	-	-	2x TC-J	-
59	-	-	2x TC-J	-
60	4x {R} Kiel Probes	Wall tap	4x {R} TC-J	3x {R} Cobra Probes

EFFECT OF HEAT EXCHANGE

The heat exchange between the flow and the case walls, and then from the wall to the surrounding environment, has been historically considered as representing the most critical factor influencing the temperature measurements inside centrifugal compressors (e.g. [1]).

More recently, however, experimental evidence of a reduced impact of this phenomenon was found in several machines tested at the test bench before their on-field installation.

In order to quantify the influence of the heat exchange between Sections 20 and 60, a comparative study was

undertaken. The temperature measurements were compared with the results of a new series of experimental studies in which a thermal insulating barrier, made with a klingerite stratus, was interposed between the diffuser walls and the inlet section of the stage to reduce the heat losses. The thermal barriers had a thermal conductivity of approximately 0.4 W/(mK), which is almost two orders of magnitude lower than that of the core material.

In addition, in order to abate the convective heat transfer between the testing cell and the surrounding environment or even the reversal of the heat flux, five heaters (Joule-effect resistors) were inserted in the case, each of which able to supply up to 3 kW: the experimental layout of the tests and the positioning of the temperature probes are shown in Figure 3. Furthermore, based on previous experiences which showed that the greater part of the heat exchange takes place between Section 20 and Section 40, specific probes were also inserted at Section 30 (i.e. middle of the diffuser), 40 and 41. Finally, several thermocouples were added to the standard instrumentation specifically to continuously evaluate the temperature of the external surface of the test bench (TC 9-14), and the case temperature (TC 1-8).

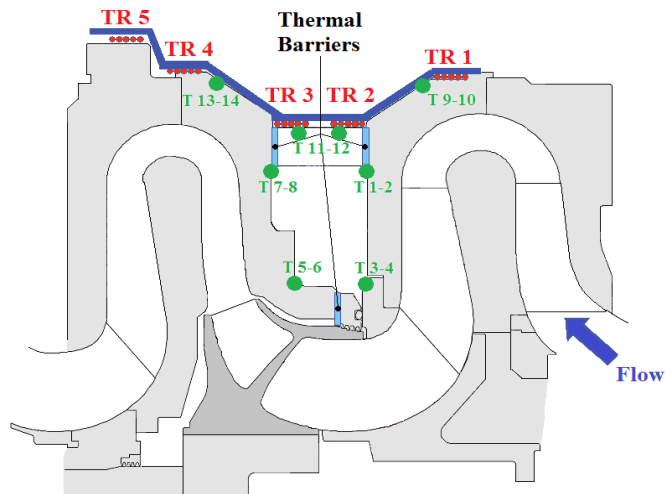


Figure 3 - Positioning of Thermal Resistors and Thermocouples.

The results of the analysis, with reference to Section 60, are reported in Figures 4 and 5. Four conditions were investigated:

- No heat flux from the heaters (blue points);
- Case temperature (T_{CASE}) maintained equal to the mean temperature in Section 20 (grey points), in which a thermal flux of 1 kW is needed from the resistors;
- Case temperature (T_{CASE}) maintained equal to the shroud temperature in Section 20 (green points) - i.e. a thermal flux of 2 kW from the resistors. The shroud temperature is the punctual temperature in the Section measured by the probe in its deepest sinking along the span;

- Power output from the heaters (red points) equal to 2.4 kW, in which a low positive heat flux is obtained.

From a perusal of the results presented in Figure 4, it is worth noticing that:

- Sections from 30 to 59 are almost unaffected by the heat flux coming from the resistors (the difference is lower than 0.2 K, which is in fact the overall uncertainty of the measurement chain). The supposed heat losses through the machine should consequently be located between Section 20 and 30.
- The measured temperatures at Section 20 (averaged temperatures along the span) are always higher than those at Section 60, therefore being independent from the external heat flux. It is worth noticing, in particular, that the temperature difference at Section 20 was increased for the condition of maximum power coming from the resistors (i.e. a local positive heat flux).

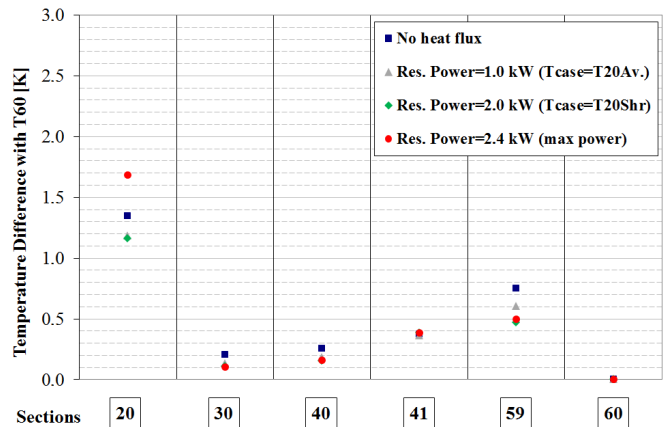


Figure 4 - Temperature Differences with T60 for different heat fluxes from the resistors - flow-path sections.

Conversely, Figure 5 reports the temperature differences between the thermocouples installed inside the chamber and Section 60. In the same figure the temperature difference with respect to the temperatures at Section 20 (average) is also reported.

Some relevant information can be deduced:

- By increasing the heat flux coming from the resistors, the same case temperatures are measured by thermocouples 1, 2, 3 and 4 (located upstream of the impeller), ensuring that a good thermal insulation was obtained with the klingerite barrier;
- T20 is only slightly lower than the case temperatures in the cavity (TC 5 and 6) measured at the same radial position than Section 20.

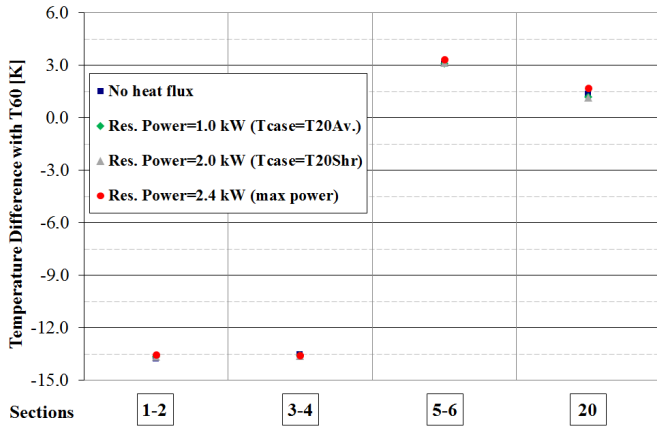


Figure 5 - Temperature Differences with T60 for different heat fluxes from the resistors - thermocouples.

Synthesizing the test results shown in Figures 4 and 5, one can conclude that hypothetical heat-losses should be concentrated only between Section 20 and 30, where a temperature difference is visible. The measured temperature of the case in that zone is not sufficient, however, to hypothesize these effects.

As a result, the total temperature discrepancy between Section 20 and 60 is only slightly affected by the heat exchange through the flow pattern.

EFFECT OF KYNETIC AND CONDUCTIVE ERROR IN THE SENSORS

The standard measurement of the total temperature made with thermocouples is affected by three sources of error in high-speed flows [1]:

- Incomplete recovery of the kinetic energy of the flow. Ideally, the sensor used for the measurement of the total temperature should be in thermal equilibrium with the temperature of the gas at rest (see Eq. 4);

$$T_0 = T + \frac{c^2}{2c_p} \quad (4)$$

- Radiating heat transfer from the sensor to the walls at a different temperature;
- Conduction through the stem of the sensor (i.e., from the sensor to the wall having a different temperature).

The design of a real total temperature probe is therefore a compromise of the three error sources [4]: indeed, as the conductive heat transfer in a gas at rest is not the preferential physical phenomenon, an excessive reduction of the velocity around the sensor (needed to pursue the optimal recovery of the kinetic energy) can lead to an enhancement of the other modes of heat transfer, such as conduction through the sensor/probe

stem and/or radiation from the sensor to the walls, thus increasing the measurement error.

As a result, an optimal velocity to be maintained around the sensor can be determined [1], which minimizes the global error in the total temperature measurement. This optimal velocity must be obtained in the surroundings of the sensor by specific flow control devices.

In particular, shielded probes are always adopted for the temperature measurement of high speed flows in turbo machines [9], having the effect of increasing the recovery of the kinetic energy, ensuring a satisfactory independence of the measurement from the angular positioning with respect to the main flow direction and reducing the radiating losses with the walls. In this study, however, the radiating contribution was purposefully neglected because shielded probes were used and relatively small temperature differences were investigated.

In order to verify the influence of the kinetic and conductive errors on the temperature difference between Section 20 and 60, a theoretical estimation of these errors was carried out. As proposed in Paniagua et al. [10], the two errors can be expressed as (Eqs. 5 and 6):

$$E_{kin} = \frac{(1-r)V_i^2}{2c_p} \quad (5)$$

$$E_{cond} = \frac{T_0 - T_{stem}}{\cosh \left[\frac{l_{wire}}{2d_{wire}} \sqrt{\frac{4Nu \cdot k_{gas}}{k_{wire}}} \right]} \quad (6)$$

where in Eq. 5, r is the *recovery factor* and V_i is the calculated velocity inside the cup of the sensor, which is derived from a mass balance (Eq. 7), where DC is the discharge coefficient and A_i the frontal area of the cup.

$$V_i = \frac{\dot{m}}{\rho_s A_i} = \frac{A_i \cdot DC \cdot Ma \cdot \frac{p_0}{\sqrt{RT_0}} \sqrt{\gamma \left(1 + \frac{\gamma-1}{2} Ma^2 \right)^{\frac{\gamma+1}{2(\gamma-1)}}}}{\rho_s A_i} \quad (7)$$

Focusing on Eq. 6, l_{wire} and d_{wire} are the length of the sensing element and its diameter, respectively; k_{wire} is the thermal conductivity of the sensor itself. Moreover, in the evaluation of the Nusselt number, the Gnielinski correlation for the forced convection in a duct was adopted [11] (Eqs. 8-9).

$$Nu = \frac{\frac{f}{2} (Re-1000) Pr}{1 + 12.7 \left(\frac{f}{2} \right)^{1/2} \left(Pr^{2/3} - 1 \right)} \quad (8)$$

$$f = (1.58 \ln Re - 3.28)^{-2} \quad (9)$$

In addition, upon examination of Eq. 6 one may note that the temperature difference between the sensing element and the stem of the probe is needed in order to correctly evaluate the conductive error. For this reason, in our study all the installed probes had an auxiliary thermocouple (J type) embedded for the acquisition of the stem temperature.

In Figures 6 and 7 the temperature corrections due to the kinetic and conductive errors at Sections 20 and 60 are reported respectively which were obtained by the application of the presented theoretical models (Eqs. from 5 to 9). In addition, in Figure 8 the corrected temperature trends at the two investigated sections as a function of the flow coefficient are shown.

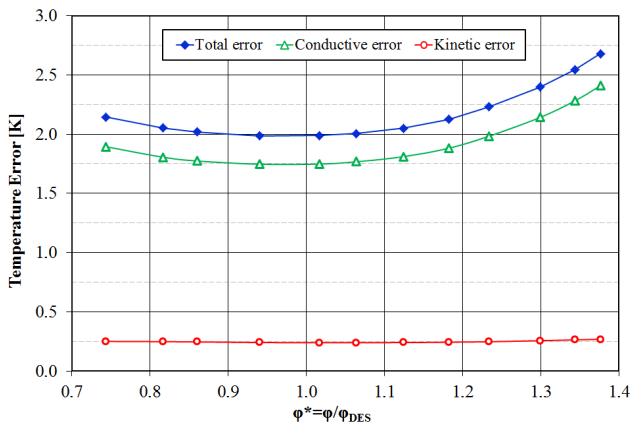


Figure 6 - Conductive and Kinetic errors at Section 20.

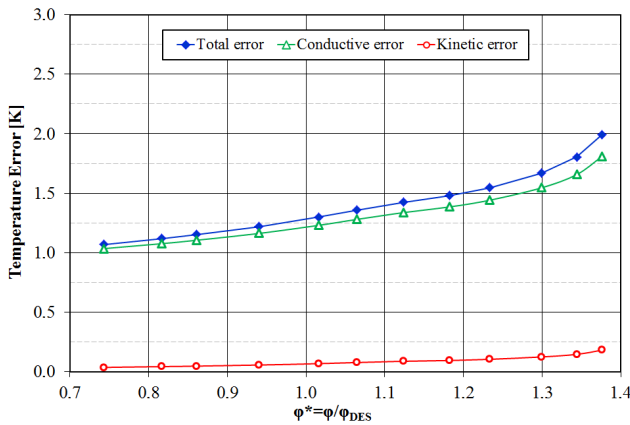


Figure 7 - Conductive and Kinetic errors at Section 60.

An analysis of the results led to some interesting remarks:

- The total error at Section 20 is constantly higher than that at Section 60, especially for low flow coefficients;
- In both sections, the main error source derives from the conductive heat exchange with the probe stem;
- The kinetic error at Section 20 is almost constant throughout the operating range and always higher than that at Section 60: the Mach number in this section is indeed

almost constant with the flow coefficient or even higher than the Mach number at Section 60;

- Focusing on Figure 8, however, (where the generic $T^* = T/T_{REF}$ and T_{REF} is T60 at the design point) one can notice that the temperature differences between the investigated sections remain almost constant after the corrections (or even higher at some operating points).

In conclusion, the kinetic and conductive errors can not be assumed to determine the temperature discrepancy between Section 20 and 60.

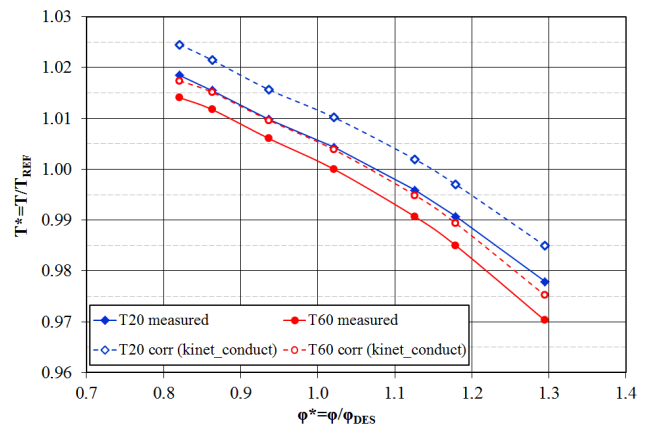


Figure 8 - Corrected temperatures due to the kinetic and conductive errors.

EFFECT OF THE FREQUENCY RESPONSE OF THERMOCOUPLES TO THE UNSTEADY FLOW

The effect of the frequency response of the temperature sensors to the unsteady flow field within the compressor, especially concerning Section 20, was then investigated in this study. The flow pattern at the impeller exit is totally three-dimensional and unstructured [2]; with a well-known scheme however, the flow structure can be described with a *jet-and-wake* approach, where the secondary zone is supposed to have an higher absolute tangential velocity than that of the primary zone and hence also a higher total temperature (Refs. [2] and [12]). Experimental high-frequency-response measurements in centrifugal compressors have confirmed the very distorted temperature distribution in the outlet region of the impeller, with a difference even higher than 20 K [13]. The hypothesis that the temperature measurement can be affected by an intrinsic error due to the frequency response of the thermocouples was then conceived [14].

More specifically, a conventional temperature sensing device, such as a thermocouple, is in this case found to respond to the highly energetic wake leaving the rotor and, due to the long thermal time constant of the probe, a temperature lying between the hot wake and the relatively cooler main stream temperature tends to be indicated. By modeling the vane with a two-zones scheme (the jet and the wake), a hypothetical temperature trend is depicted in Figure 9.

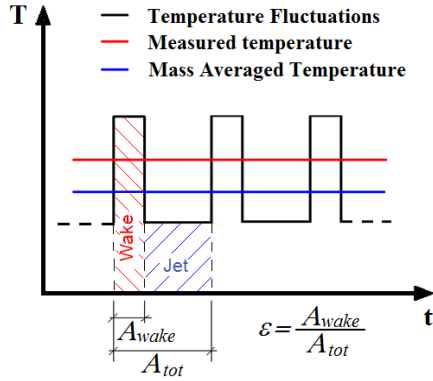


Figure 9 - Hypothetical temperature measurement of a thermocouple in a pulsating flow.

Within this scheme, the temperature level indicated by the thermocouple could be closer to the time averaged mean (red line) than to the mass-flow averaged mean (blue line) with a general overestimation of the measured quantity.

A model to account for this effect was proposed by Olczyk [14] for an axial compressors and, in our study, an application of this model to centrifugal compressors is proposed. The heat exchange between the gas and the sensor can be simply described by Eq. 10, where X is a semi-empirical factor which is function of the shield's shape and of the surrounding flow conditions: in this study, an X value equal to 1 was selected because all the probes were aligned to the flow before the acquisition.

$$Q = h_c X (T_{gas} - T_s) \quad (10)$$

In the proposed application of the model, Eq. 10 was considered as quasi-steady, i.e. the net heat exchange between the sensor and the flow is regulated by the instantaneous value of the two temperatures and of the convective coefficient h_c .

This assumption implies however the consideration of a quasi -steady behavior of the boundary layer which regulates h_c .

Due to the high-velocity fluctuations of the flow which impinge on the sensor, the internal conduction in the sensor itself was also neglected; Eq. 10 can be consequently re-written after integration over a period T as:

$$\int_t^{t+T} Q dt = \int_t^{t+T} h_c X T_{gas} dt - \int_t^{t+T} h_c X T_s dt \quad (11)$$

After an initial transitory, the sensor is supposed to reach the quasi-steady state. The first term of Eq. 11 can therefore be neglected, yielding Eq. 12:

$$(h_c X T_{gas})_{TA} = (h_c X T_s)_{TA} \quad (12)$$

where the subscript TA indicates a Time-Averaged quantity. If one hypothesizes that the response of the sensor is

sufficiently short to correctly follow the temperature fluctuations, the discrepancy between T_{air} and T_s is supposed to be almost negligible and Eq. 12 is constantly verified. In reality, however, the thermal inertia of the thermocouple introduces a mismatch between the real temperature and the measured value. This latter value can therefore be expressed as:

$$T_s = \frac{(h_c X T_{gas})_{TA}}{(h_c X)_{TA}} \quad (13)$$

In this model the resulting error between T_{gas} and T_s is null for the pulsation frequencies which can be correctly followed by the sensor and goes up to that of Eq. 13 for higher frequencies, where the frequency response of the thermocouple becomes too slow to capture the temperature ripples.

By assuming that the wake zone repeats itself as a square-wave signal (see Figure 9) for a spatial extension equal to ε part of the vane, the time-averaged temperature sensed by the thermocouple, obtained by Eq. 13, becomes:

$$T_s = \frac{X_j h_j (1 - \varepsilon) T_j + X_w h_w \varepsilon T_w}{X_j h_j (1 - \varepsilon) + X_w h_w \varepsilon} \quad (14)$$

where the j and w subscripts indicate the jet and the wake zones, respectively. Defining now X' as:

$$X' = \frac{X_w h_w}{X_j h_j} \quad (15)$$

Eq. 14 becomes:

$$T_s = \frac{\varepsilon(1 - \varepsilon)(1 - X')(T_w - T_j)}{1 - \varepsilon(1 - X')} \quad (16)$$

With the same considerations, the real time-averaged temperature of the flow and the difference between the real and the measured become, respectively:

$$T_{gas} = (1 - \varepsilon)T_j + \varepsilon T_w \quad (17)$$

$$\Delta T_{TA} = \frac{\varepsilon(1 - \varepsilon)(1 - X')(T_w - T_j)}{1 - \varepsilon(1 - X')} \quad (18)$$

From a machine point-of-view however, a more coherent approach to evaluate the average temperature of the flow should be based on a mass-averaging process. In this approach, the mass-averaged flow temperature becomes:

$$T_{MA} = \frac{(1 - \varepsilon)T_j V'_j \rho_j + \varepsilon T_w V'_w \rho_w}{(1 - \varepsilon)V'_j \rho_j + \varepsilon V'_w \rho_w} \quad (19)$$

where V' indicates the meridian velocity component. Defining now:

$$\hat{V} = \frac{V'_w \rho_w}{V'_j \rho_j} \quad (20)$$

Eq. 19 becomes:

$$T_{MA} = \frac{(1-\varepsilon)T_j + \varepsilon\hat{V}T_w}{1-\varepsilon(1-\hat{V})} \quad (21)$$

The error which affects the measurement of the sensor in a mass-averaged approach is therefore given by:

$$\Delta T_{MA} = T_{MA} - T_s = \frac{\varepsilon(1-\varepsilon)(\hat{V} - X')(T_w - T_j)}{(\varepsilon X + 1 - \varepsilon)(\varepsilon\hat{V} + 1 - \varepsilon)} \quad (22)$$

Upon examination of Eq. 22, one can notice that with the correct sensor data and an in-depth study of the flow parameters (i.e., by imposing X' , \hat{V} and ε) a correction of the measured value of the thermocouple can be obtained.

In this study, a specific analysis was carried out to define the jet and wake portions inside a vane. To this purpose, a combined experimental-numerical approach was again applied. The 1D *Compal* software (e.g. Refs. [15,16]) was in fact first calibrated with the experimental data collected for the investigated compressor at the design point, obtaining constant agreement between the numerical estimations and the experimental data on all of the investigated parameters (for further details see Ref. [13]).

As a second step, the experimental data obtained in a series of tests with a *Fast Response Pressure Probe (FRAPP)* [13] were exploited to create 2D maps of the *rothalpy loss coefficient* ζ , defined as (Eq. 23):

$$\zeta = \frac{P_{0\omega 1} - P_{0\omega 2}}{P_{0\omega 1} - P_1} \quad (23)$$

where:

$$P_{0\omega} = P \left(\frac{T_{0\omega}}{T} \right)^{\frac{\gamma}{\gamma-1}} \quad (24)$$

$$T_{0\omega} = T + \frac{1}{2c_p} (W^2 - U^2) \quad (25)$$

The rothalpy loss coefficient can in fact be used as an effective index to separate the jet and wake regions (Refs. [17,19]), in which nearly all the losses are located. In particular, the ζ map at the design point (Figure 10) was reduced to a dimensionless form by the ζ^* parameter (Eq. 26) and consequently analyzed by means of an image-processing software in order to find the contour line which divided the map itself into jet and wake regions corresponding to the ε ratio obtained with the *Compal* code (i.e. the bold contour at

$\zeta^*=0.48$ in Figure 10), on the assumption that the code is fully predictive at the design point.

$$\zeta^* = \frac{\zeta - \zeta_{MIN}}{\zeta_{MAX} - \zeta_{MIN}} \quad (26)$$

Since the ζ^* value is scaled on each map (i.e. reduced with the minimum and maximum values of each map), the chosen contour was assumed to represent the boundary line between the jet and wake regions for all the operating conditions of the compressor.

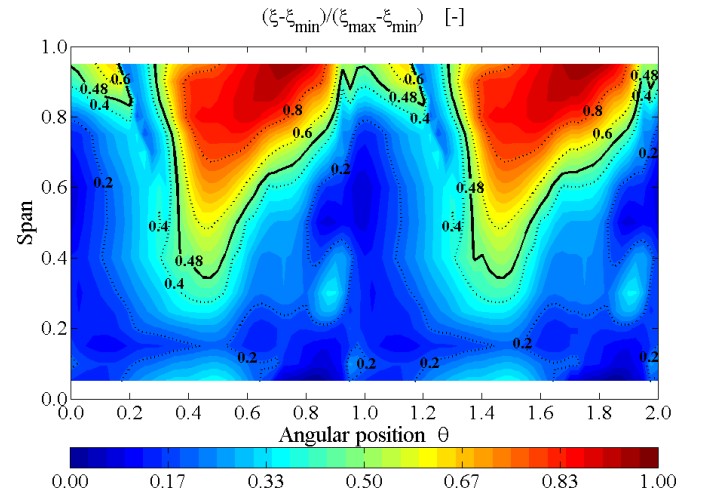


Figure 10 - ζ^* map at the design point.

Based on these assumptions, the ε ratio was calculated using the experimental pressure maps as a function of the flow coefficient, whose trend is reported in Figure 11. It is worth noticing that a sensitivity analysis was carried out to evaluate the influence of the ζ^* definition on the resulting ε ratio, obtaining that the approach followed can in fact clearly define the two zones, i.e. a reduced influence of loss-coefficient variations was found on the calculated ε ratio.

Finally, in order to apply the above discussed model for the correction of the measured temperature, some other assumptions were made:

- The Gnielinski correlation for convective heat exchange (Eqs. 8 and 9) was adopted;
- The *Compal* estimations were used to evaluate all the thermodynamic quantities required for the model (i.e. temperature, density and velocity of the jet and wake regions, Mach numbers) and, in particular, the temperature of the jet and wake regions;
- The meridian velocities in the two zones were calculated by means of the Mach maps obtained with the FRAPP probe and the temperatures derived from the model (for further information on the experimental data acquisition and results see Refs. [13] and [20]).

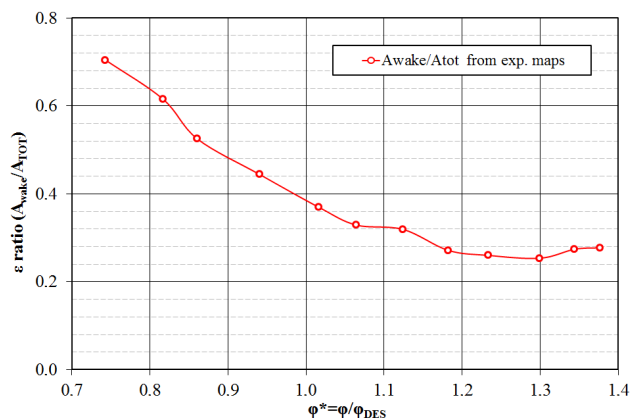


Figure 11 - Calculated ε ratios.

Within these assumptions, the corrected temperatures at Section 20 due to the effects on the measurement of the jet-and-wake structure of the flow are presented in Figure 12.

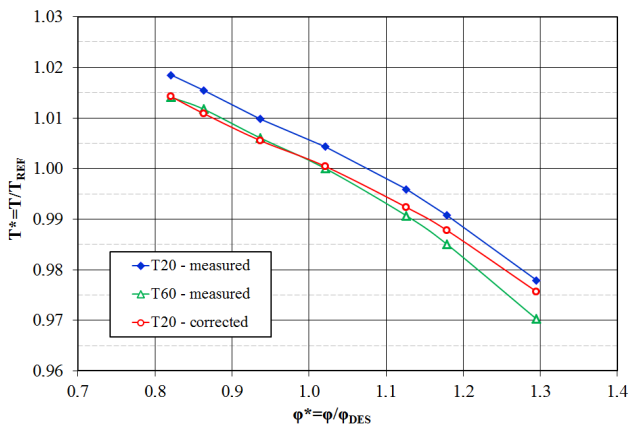


Figure 12 - Comparison of temperatures after correction to account for the jet-and-wake structure of the flow.

The correction applied to account for the pulsating structure of the flow at Section 20 seems to correctly explain the discrepancy between the measured temperatures at the impeller outlet section and at the stage exit section.

In particular, noticeable agreement between the corrected values at Section 20 and the measured values at Section 60 was found both at the design flow coefficient and for lower ϕ values, whereas the correction was not completely adequate for higher ϕ values.

In the authors' opinion, this latter trend must be connected to some uncertainties on the evaluation of the temperature difference between the wake and jet zones made by the *Compal* code, which was calibrated only at the design point. More specifically, the numerical predictions for higher flow coefficients generally showed a lower agreement with the experimental data also concerning the overall performance of the machine and consequently errors on the evaluation of the wake and jet temperatures were probably introduced in the

analysis; in fact, a significant influence of these temperatures on the deriving correction was noticed.

In order to overcome this problem, an in-depth study on these effects has been planned for the near future, most likely by means of experimental techniques to measure the real mean temperatures of the wake and jet regions, respectively.

Although further studies are required to verify the analyzed trend, the jet-and-wake structure which incomes on the thermocouple at Section 20 has been apparently deemed to induce an error in the correct evaluation of the total temperature in this section, with a general overestimation of the physical value.

As a result, in order to promote a standardization of the testing protocols, the total temperature at Section 60 can be actually considered as the most reliable reference for the estimation of the performance of the whole compressor.

CONCLUSIONS

This study reports an in-depth examination of the influence on the performance estimation of a centrifugal compressor of the considered section for the measurement of the total temperature

Based on the experimental evidence of a discrepancy between the measured temperatures at the impeller outlet section and at the stage exit section, a combined experimental and theoretical approach was carried out to evaluate the relative impact of three physical phenomena which were hypothesized to affect the measurements.

In particular, specific experimental tests undertaken on a high pressure impeller showed that the heat exchange between the flow and the case along the flow path has a very slight influence on the temperature difference between the two sections and is not sufficient to explain the phenomenon. Furthermore, the kinetic and conductive measurement errors on the probe have a real impact on the measured quantity but their influence is almost equal in the investigated sections, not being actually influent on the temperature difference between the impeller outlet section and at the stage exit section.

Finally, the totally three-dimensional and unstructured flow at the impeller outlet was assumed to induce measurement errors in the temperature estimation at Section 20, due to the inadequate frequency response of the thermocouple in unsteady flow. As a consequence, a correction model was applied to the measured valued at Section 20 by means of both numerical estimations and experimental data derived from a Fast Response Pressure Probe.

Notable agreement was found between the corrected temperatures at Section 20 and the measured temperatures at Section 60, suggesting that the total temperature at Section 60 can be considered as the most reliable reference for the estimation of the performance of the whole compressor.

ACKNOWLEDGMENTS

Thanks are due to Professor Ennio Antonio Carnevale of the University of Florence for supporting this activity.

The authors would also like to acknowledge Dott. Giuseppe Sassanelli and Dott. Stefano Cioncolini of *GE Oil & Gas* for the helpful discussion and their invaluable contribution to this study.

REFERENCES

- [1] Manfrida, G., Fiaschi, D., and Tapinassi, L., 2006, "Improving the Accuracy of Tests for Centrifugal Compressor Stage Performance Prediction," *Proc. ASME-ESDA Engineering Systems Design and Analysis*, Torino, Italy, July 4-7, 2006, pp. 20-29.
- [2] Cumpsty, N. A., 1989, *Compressor Aerodynamics*, Krieger Publishing, New York, USA.
- [3] Busemann, A., 1928, "Das Forderhohenverhältnis radialer Kreiselpumpen mit logarithmisch-spiraligen Schaufeln," *Zeitschrift fuer angewandte Mahtmatik und Mechanik*, **8**, pp. 372-384.
- [4] Moffat, R.J., 1962, *Gas Temperature Measurement, Temperature - Its Measurement and Control in Science and Industry*, Rheinold, New York, USA, pp. 553-571.
- [5] Bidini, G., Manfrida, G. and Valentini, E., 1987, "Assessment of Measurement Error for Gas-Turbine Total Temperature Probes," *Proc. Fluid Measurement and Instrumentation Forum*, Cincinnati, USA, June 14-17, 1987, **49**, pp. 23-26.
- [6] Agnew, B., Elder, H., and Terrel, M., 1985, "An Investigation of Response of Temperature Sensing Probes to an Unsteady Flow Field," *Proc. ASME International Gas Turbine Conference and Exhibit 30th*, Houston, USA, June, 1985.
- [7] Ferrara, G., Ferrari, L., Mengoni, C. P., De Lucia M. and Baldassarre, L., 2002, "Rotating Stall In Centrifugal Compressor with Vaneless Diffuser: Experimental Analysis And Phenomenon Characterization," *Proc. 9th of International Symposium on Transport Phenomena and Dynamics of Rotating Machinery*, Honolulu, USA, February 10-14, 2002.
- [8] Barigozzi, G., Dossena, V. and Gaetani, P., 2000, "Development and First Application of a Single Hole Fast Response Pressure Probe," *Proc. XV Symposium on Measuring Techniques in Transonic and Supersonic Flows in Turbomachines*, Florence, Italy, September 23-24, 2000.
- [9] Doebelin, E.O., 2003, *Measurement systems: application and design*, McGraw-Hill, Boston, USA, 5th ed.
- [10] Paniagua, G., Dénos, R. and Oropesa, M., 2002, "Thermocouple Probes For Accurate Temperature Measurements In Short Duration Facilities," *Proc. of the ASME TURBO EXPO 2002: Power for Land, Sea, and Air (GT2002)*, Amsterdam, The Netherlands, June 3-6, 2002.
- [11] Kreith, F. and Bohn, M., 2001, *Principles of Heat Transfer*, Thomson Learning, New York, USA, 6th edition.
- [12] Mansour, M., Chokani, N., Kalfas, A. and Abhari, R., 2007, "Unsteady Entropy Measurements In A High-Speed Radial Compressor," Paper no. GT2007-27450, *Proc. ASME Turbo Expo 2007: Power for Land, Sea, and Air (GT2007)*, Montreal, Canada, May 14-17, 2007.
- [13] Toni, L., Ballarini, V., Cioncolini, S., Gaetani, P., and Persico, G., 2010, "Unsteady Flow Field Measurements in an Industrial Centrifugal Compressor," *Proc. Thirty-Ninth Turbomachinery Symposium*, Houston, USA, October 4-7, 2010, pp. 49-58.
- [14] Olczyk, A., 2008, "Problems Of Unsteady Temperature Measurements In A Pulsating Flow Of Gas," Paper 055402, *Measurement Science And Technology*, **19**(5).
- [15] Howard, J.H.G. and Osborne, C., 1977, "A Centrifugal Compressor Flow Analysis Employing a Jet-Wake Passage Flow Model," *Journal of Fluids Engineering*, **99**(1), pp. 141-148.
- [16] Qiu, X., Mallikarachchi, C. and Anderson, M., 2007, "A New Slip Factor Model for Axial and Radial Impellers," Paper no GT2007-27064, *Proc. ASME Turbo Expo 2007: Power for Land, Sea, and Air (GT2007)*, Montreal, Canada, May 14-17, 2007.
- [17] Dean, R.C. and Senoo, Y., 1960, "Rotating wakes in vaneless diffusers," *Transactions ASME, Series D*, No. 5, pp. 563-574.
- [18] Denton, J.D., 1993, "Loss Mechanisms in Turbomachines," *Journal of Turbomachinery*, **115**(4), pp. 621-657.
- [19] Britton, I. and Gauthier, D., 2008, "Performance Prediction of Centrifugal Impellers Using A Two-Zone Model," Paper no GT2008-51530, *Proc. ASME Turbo Expo 2008: Power for Land, Sea, and Air (GT2008)*, Berlin, Germany, June 9-13, 2008, pp. 1695-1704.
- [20] Guidotti, E., Tapinassi, L., Toni, L., Bianchi, L., Gaetani, P. and Persico, G., "Experimental and Numerical Analysis of the Flow Field in the Impeller of a Centrifugal Compressor Stage at Design Point," Paper no GT2011-45036, presented for publication at the *ASME Turbo Expo 2011 (GT2011)*, Vancouver, Canada, June 6-11, 2011